

# Enhanced Supercritical CO<sub>2</sub>-Water Phase Contact via Electrodispersion

Kevin D. Heath and Hank D. Cochran \*

Chemical Technology Division  
Oak Ridge National Laboratory  
Oak Ridge, TN 37831-6224

and Chemical Engineering Department  
University of Tennessee  
Knoxville, TN 37996-2200

hdc@ornl.gov; fax 865-241-4829

Supercritical carbon dioxide is a preferred solvent substitute in the chemical process industries, but processing which requires contact between CO<sub>2</sub> and an aqueous phase has been hindered by the inefficient phase contact and high capital cost of conventional contactors. We examine the phase-contact performance of an electrodispersion contactor in this service. We have dispersed droplets of aqueous phases into supercritical CO<sub>2</sub> using pulsed, high-intensity electric fields. Using small angle laser light scattering, we characterized the mean droplet size as a function of operating conditions (liquid flow rate, field strength, frequency, temperature, and pressure) and observed operating regions that yield submicron-sized droplets. The effects of temperature and pressure on droplet size were correlated with the interfacial tension. Then, using the extraction of ethanol from a water-ethanol solution as a test system, we attempted to characterize mass transfer performance, but under maximum CO<sub>2</sub> flow rate conditions of the downstream liquid condensers, mass transfer was equilibrium limited in all cases. Because of the small droplet size and high interfacial area, the electrodispersion contactor offers the potential to achieve excellent mass transfer performance. The submicron-sized droplets were efficiently coalesced electrostatically, and negligible entrainment was observed. We anticipate that initial commercial applications might be for processing small volumes of high-value substances in aqueous media such as might be found, for instance, in the pharmaceutical industry.

## Introduction.

Processing of aqueous streams with supercritical carbon dioxide (SC-CO<sub>2</sub>) will usually require mass transfer between the liquid aqueous phase and the SC-CO<sub>2</sub> phase. Conventional phase contactors such as packed beds or plate columns may be inefficient in such applications; the pressure drop required may affect phase behavior; and pressure vessels for such conventional contact may be costly. In this paper we describe exploratory experiments in which an aqueous phase is finely dispersed as submicron-sized droplets into SC-CO<sub>2</sub> using a pulsed, high-intensity electric field. The principle of operation, electrospraying, has previously been employed for spraying liquid into ambient air, for example, in ink-jet printing. In this introduction we will briefly review prior research on electrospraying. Then, in the next section, we will describe our apparatus and the experiments we have performed. We will present our results on droplet size

characterization as a function of operating parameters and then our results on extraction of ethanol from an ethanol-water mixture. Finally, we will present some brief concluding remarks.

Over the past fifteen years, researchers have explored drop and bubble formation behavior in electric fields from fundamental and applied perspectives. Techniques have been developed for producing aqueous dispersions in non-conducting organic solvents using intense electric fields; these developments have resulted in patents for an emulsion phase contactor to be used in separations<sup>1,2</sup> and for an electric dispersion reactor.<sup>3-5</sup> A number of applications have been explored,<sup>6-13</sup> and successful technology transfer has resulted in commercialization. To date the solvents in which the submicron-sized dispersions have been produced have included many organic liquids but never dense, compressible supercritical fluids. The goal of this work was to test feasibility of this technique, which would broaden the range of separation and reaction processes in which SC-CO<sub>2</sub> is applicable.

Electrospraying is a process that relies on electrical forces to break a liquid into fine, charged droplets. One of the simplest ways of implementing such a process is to feed a liquid with sufficient electric conductivity through a grounded metal capillary a few centimeters away from a conducting mesh screen, which is charged to a sufficiently high electric potential. Under the influence of the electric field, the liquid may emerge in different flow modes: dripping, microdripping, cone-jet, spindle, simple jet, and ramified jet. In the cone-jet mode, the liquid forms a cone-shaped interface at the outlet of the capillary. Through the apex of the cone, a fine thread of liquid is ejected, which breaks into monodisperse droplets because of capillary instability.<sup>14-17</sup> When the mode of electrospraying extends past the cone-jet mode into the spindle, simple jet, or ramified jet mode, monodispersity is no longer observed as instabilities at the liquid apex cause a large range of different droplet sizes to be emitted. The applied voltage is a key parameter in establishing the cone-jet mode; various modes of spraying can be observed depending on the voltage applied.<sup>15-17</sup> However, droplet size has been reported to be virtually independent of the applied voltage for liquids of relatively high electrical conductivity.<sup>18,19</sup> Tang and Gomez<sup>20</sup> observed that at low flow rates, the applied voltage seems to have a modest effect, and at larger flow rates, the droplet size decreases almost linearly with the increase of the applied voltage. This effect appears to be more pronounced for lower conductivity solutions. Within the range of applied voltage that ensures a stable cone-jet, as much as 50 % reduction in size was observed for a fixed flow rate of the lower conductivity solution. If the mode of electrospray is

beyond the cone-jet mode, polydispersity is observed, and an increase in droplet size can be seen upon increasing the field strength.<sup>15</sup>

The frequency of a pulsed electric field affects the size of the droplets<sup>21,22</sup> as well. The most interesting behavior is found to occur when the electric field pulse frequency is in the vicinity of the natural oscillation frequency of the droplet.<sup>23</sup> Near this natural frequency, a significant increase in field strength is required for droplet rupture;<sup>21</sup> hence, this implies that this is the condition of maximum stability for the droplet. In addition, stability of the droplet drastically decreases on either side of the natural frequency.

### The Electrodispersion Contactor.

The central component in the experimental apparatus is a high-pressure electrodispersion contactor (EDC). The pressure vessel is a view cell obtained from Pressure Products Industries, Inc., capable of operating at pressures up to 34.47 MPa and temperatures from -30 to 175 °C. An EDC was fabricated from this pressure cell by installing fluid supply and withdrawal lines, electrical feedthroughs, and internal electrodes (see Figure 1). The inside chamber is in the shape of a cylinder with a diameter of 5.08 cm and a height of 17.78 cm.

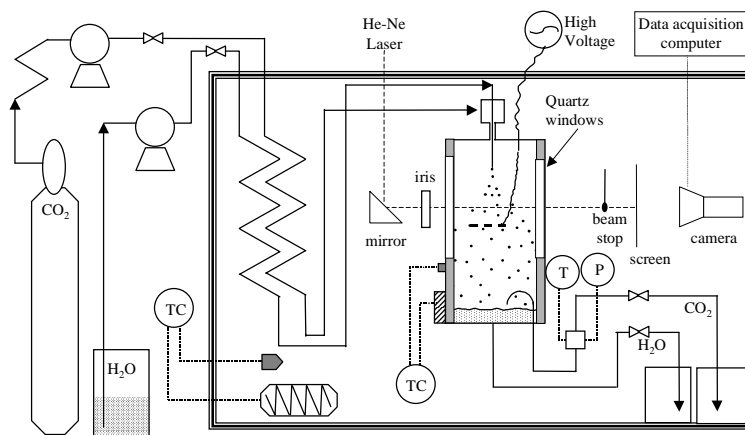


**Figure 1.** Schematic diagram of EDC apparatus.

Flow of water or other aqueous liquid is established through a grounded, tapered 1.59 mm OD capillary tube with a SSI 222C high-pressure liquid chromatograph (HPLC) pump, and the level of accumulated liquid in the cell is maintained by adjusting the water let down valve (Autoclave Eng., micrometering valve 30VRMM4812). The CO<sub>2</sub> flow is established with a

Teledyne Sprague Engineering Model S-86-JN-60 booster compressor; the pressure of the system is maintained by adjusting the CO<sub>2</sub> let down valve (Autoclave Eng., micrometering valve 30VRMM4812). For the recovery of extract, the CO<sub>2</sub> outlet stream is sent to a series of U-tube condensers (1.27 cm OD and 0.635 cm ID), which contain glass wool for increased effectiveness. A Fisher Porter gas flow meter is used for online flow rate indication, and a wet test meter (Singer American Meter Division Model 802, serial no. P-843) is used for precise volumetric flow measurement of the CO<sub>2</sub> outlet stream. A bypass valve is located before the condensers so that the system can reach steady state before the condensers are operated. System operation proved to be simple and stable so that controlled electrodispersion experiments could be performed successfully.

A custom-built pulsed dc voltage generator (see Figure 2) created the electric field. This generator utilizes a Global Specialties 4001 pulse generator and an Electronics Measurements, Inc., SCR dc power source that are supplied to a custom built pulser. The pulser then energizes a 12 V dc automotive high-voltage coil (Mallory Promaster). The coil produces the high voltage, which is sent through high-voltage diodes (Collmer Semiconductor, Inc., CS4107X30) to a stainless steel screen 2.5 cm in diameter and 2.5 cm below the grounded feed capillary. The

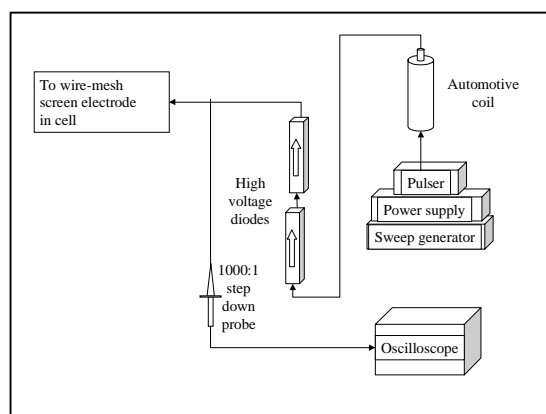


**Figure 2.** Electrical schematic for providing pulsed, high-voltage electric fields.

voltage is measured using a high-voltage step-down probe (Farnell HV40B; 1000:1) coupled with a Tektronix Inc., Type 504 oscilloscope to accurately determine the optimum voltages and frequencies. The oscilloscope was calibrated to within 2%, less than the width of the trace line. This system is capable of pulses up to 30 kV at 0-10 kHz. Except under conditions of electrical

breakdown and arcing, the electric current drawn by the EDC was negligible. Prior experience<sup>1-13</sup> indicates that power consumption by the EDC in applications will be small compared with that required for dispersion in conventional contactors.

The EDC was operated with an aqueous liquid and CO<sub>2</sub> flowing in a co-current mode. The carbon dioxide and liquid entered the cell through ports in the top with no pre-mixing. There are two outlet ports, one for draining the accumulated aqueous solution, the second, an extended crooked sheltering tube for CO<sub>2</sub> removal. The pressure of the system was measured with an analog gauge supplied by Sprague Engineering Corp. with an accuracy of  $\pm 0.34$  MPa. An air bath with a high-intensity circulating fan was used to control temperature and minimize electrical hazards. Since the cell consists of an almost solid block of stainless steel with an approximate weight of 34 kg, a separate electrical resistance heater (Omegalux, 505/5-P) and digital temperature controller (Omega; custom built) have been adapted to the cell itself to assist in temperature control. Temperature control was maintained to  $\pm 0.1$  °C.

To characterize mean droplet size, a laser light scattering system was used. A 10-mW He-Ne laser was positioned to enter the cell through a contractible iris to control the beam diameter and to block extraneous light. On exiting the cell, the high intensity of the beam was blocked with a beam stop, and the remaining scattered light was displayed on a screen designed especially for uniformity. The image of the scattered light on the screen was then acquired through a video camera (Pulnix TM-200) and sent to a DigitalVision RT Mono frame grabber for computer analysis. A two dimensional profile of intensity versus distance from the center of the beam was created based on the observed pattern on the screen. For analysis, these data were converted to light intensity versus the magnitude of the scattering vector. Monodispersed samples of 10 and 2  $\mu\text{m}$  sizes were used for calibration. For the data analysis, the distribution of aqueous droplets in the EDC has been assumed to be Lorentzian, and the droplets have been assumed to be spherical.

### **Droplet Size.**

Prior to quantitative experiments determining droplet size, a series of exploratory experiments was performed to determine operating conditions in which the water feed stream to the EDC would be finely dispersed by the pulsed electric field. This was accomplished by establishing pressure, temperature, and flow rates with the electric field off. The flow was visually

observed. Then, the pulsed field was turned on, and the flow mode was observed again. We considered that the EDC was producing finely dispersed droplets when, upon turning on the field, the droplets were so small that they were no longer visible to the eye. Such fine aqueous dispersions were only found under the field-on conditions. All of the results reported below were obtained under these operating conditions.

The series of frames in Figure 3 displays the effect of increasing the water flow rate to the EDC while maintaining a constant voltage of -8.8 kV (3.5 kV/cm), pressure (7.58 MPa), temperature (40°C), and frequency (400 Hz). Figure 3a uses a flow rate of 4.0 ml/min; Figure 3b, 5.0 ml/min; while the last, Figure 3c, 6.0 ml/min. The dispersion effect remains in all three cases. The only noticeable difference between the three is the extension of the initial stream length. This shows that the process is feasible over a range of flow rates. The limit of the dispersion is balanced by the flow of the aqueous solution and the electric field, which shatters it. The mode of electrospray for this figure appears to be that of the ramified jet,<sup>15</sup> characterized by the liquid thread widening at the apex and its edges emitting many fine jets.

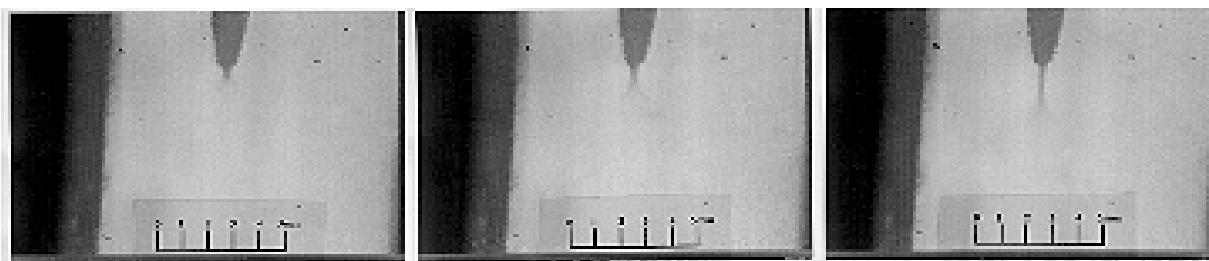


**Figure 3.** Series of frames depicting the effect of increasing the aqueous flow rate on a dispersion into supercritical CO<sub>2</sub> at 40°C, 3.5 kV/cm, and 400 Hz. (a) 4.0 ml/min, (b) 5.0 ml/min, (c) 6.0 ml/min. Inserted scale is 5 mm with each division being 1 mm.

Figure 4 shows the relationship of field strength (2-5 kV/cm) and mean droplet diameter  $\langle d_p \rangle$  for three pulse frequencies (100, 1,000, and 10,000 Hz) while holding the water flow rate constant at 3 ml/min. Here  $\langle d_p \rangle$  increases with increasing field strength. Specifically an increase from 0.9  $\mu\text{m}$  at 2 kV/cm to 1.75  $\mu\text{m}$  at 5 kV/cm was observed. This result appears contrary to prior work in the cone-jet mode,<sup>24</sup> but likely this result and those in the following paragraphs were not obtained in the cone-jet mode. Prior work has established that increasing the field strength while in the cone-jet mode causes a decrease in droplet size. However, an electrospray which operates beyond the onset of cone-jet mode (at higher field strength, flow rate,

or both) becomes unstable and polydisperse. Polydispersity is believed to have caused the observed increase in  $\langle d_p \rangle$  with increasing field strength seen in Figure 4. The results in Figure 4 also show the effect of increasing the pulse frequency. All three pulse frequencies give similar  $\langle d_p \rangle$  at lower field strength with higher frequency giving a larger  $\langle d_p \rangle$  at higher field strength.

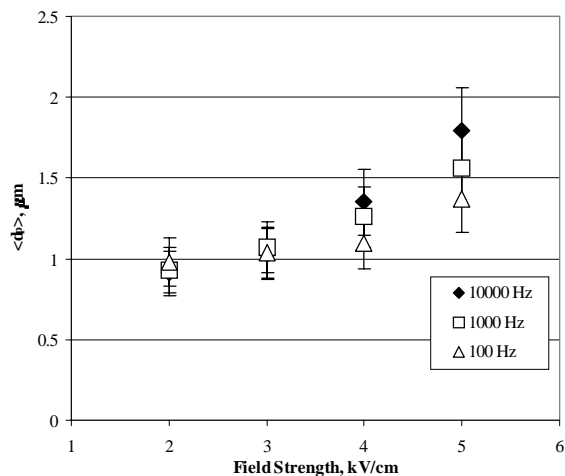
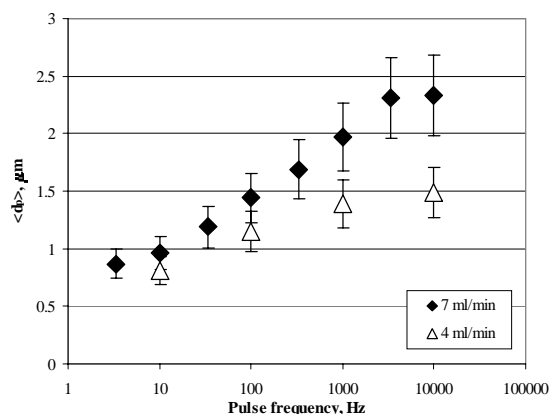


**Figure 4.** Effect of field strength on  $\langle d_p \rangle$  with distilled H<sub>2</sub>O at flow rate of 3 ml/min, 10.34 MPa, and 40°C.

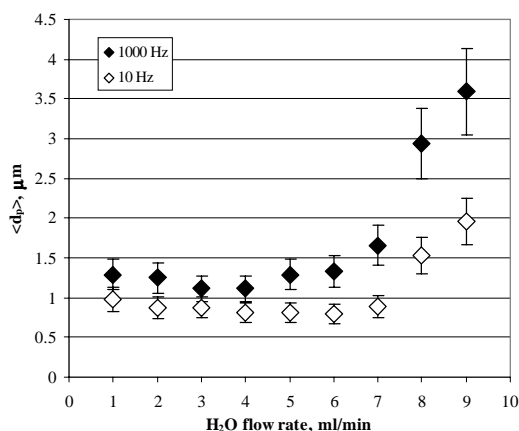
Figure 5 displays the effect of increasing pulse frequency (1-10,000 Hz) on  $\langle d_p \rangle$  for two water flow rates (4 and 7 ml/min) while holding the field strength constant at 4 kV/cm. Here it is shown, that at the lower pulse frequency of 10 Hz,  $\langle d_p \rangle$  is smaller than 1.0  $\mu\text{m}$  for both flow rates. However, as the pulse frequency is increased to 10,000 Hz, the  $\langle d_p \rangle$  for both flow rates increase. The 7 ml/min data set shows a larger dependence with an increase to 2.3  $\mu\text{m}$  for increased pulse frequency, while the 4 ml/min data set has a more modest dependence with a  $\langle d_p \rangle$  of 1.5  $\mu\text{m}$  at the highest pulse frequency.

Figure 6 gives the effect of increasing flow rate (1-9 ml/min) on  $\langle d_p \rangle$  for two pulse frequencies (10 and 1,000 Hz) while holding the field strength constant at 4 kV/cm. At lower water flow rates (1-6 ml/min),  $\langle d_p \rangle$  appears fairly constant for these conditions, but increases once the flow increases. For all flow rates the 10 Hz data set gives smaller  $\langle d_p \rangle$  than the 1,000 Hz data set. The 10 Hz data set shows  $\langle d_p \rangle$  less than 1.0  $\mu\text{m}$  until a flow rate of 8 ml/min where it climbs to 1.5  $\mu\text{m}$  with a maximum of 2  $\mu\text{m}$  at 9 ml/min. For the 1,000 Hz data set the  $\langle d_p \rangle$  stays below 1.5  $\mu\text{m}$  until the flow rate is raised to 8 ml/min where it increases to almost 3  $\mu\text{m}$

with a maximum of 3.5  $\mu\text{m}$  at 9 ml/min. Findings of increased  $\langle d_p \rangle$  with increasing flow rate similar to these have been observed by many researchers<sup>15-20,24</sup> for electro spraying liquid into gas.



**Figure 5.** Effect of pulse frequency on  $\langle d_p \rangle$  at 4kV/cm, 10.34 MPa, and 40°C for distilled H<sub>2</sub>O.



**Figure 6.** Effect of flow rate on  $\langle d_p \rangle$  at 4kV/cm, 10.34 MPa, and 40°C for distilled water.

Figures 7a-c present the effects of liquid flow rate, temperature, and pressure on  $\langle d_p \rangle$  in electrodispersion of 10 vol. % aqueous ethanol in SC-CO<sub>2</sub>. Temperatures of 35, 47, and 65°C, pressures of 10.34, 13.79, and 17.24 MPa, and flow rates of 2-12 ml/min were examined at constant field strength (2.7kV/cm) and constant pulse frequency (133 Hz). An attempt to understand the data is presented with a focus on surface tension, one of the several physical properties that change with state conditions.

Figure 7a displays the effect of temperature (35, 47, and 65°C) on  $\langle d_p \rangle$  at a constant pressure of 10.34 MPa. The 35°C data set has  $\langle d_p \rangle$  that are almost all less than 1.0  $\mu\text{m}$  at all liquid flow rates from 2-12 ml/min. At 10.34 MPa, increasing the temperature causes an increase in  $\langle d_p \rangle$  over all flow rates. Figure 8 displays the effect of temperature (35, 47, and 65°C) on  $\langle d_p \rangle$  at a constant pressure of 13.79 MPa. All the temperatures at this pressure exhibit similar  $\langle d_p \rangle$  especially at the lower flow rates from 2-6 ml/min. At higher flow rates (8-12 ml/min), the 35°C data set has the largest  $\langle d_p \rangle$  at 2.4  $\mu\text{m}$  for 12 ml/min flow. In Figure 7b, the 65°C data set has the smallest  $\langle d_p \rangle$  at 1.6  $\mu\text{m}$  for 12 ml/min flow. There exists a slight dependence (increase of  $\langle d_p \rangle$ ) with flow rate for all three temperatures at this pressure. Figure 7c displays the effect of temperature (35, 47, and 65°C) on  $\langle d_p \rangle$  at a constant pressure of 17.24 MPa. This plot shows the

reverse effect of that observed for the 10.34 MPa data set. The lowest temperature (35°C) now produces the largest  $\langle d_p \rangle$ , while the highest temperature (65°C) gives the lowest  $\langle d_p \rangle$ . The 65°C data set shows a very weak dependence of  $\langle d_p \rangle$  on liquid flow rate ranging from 1.1  $\mu\text{m}$  at 2 ml/min to 1.3  $\mu\text{m}$  at 12 ml/min. While the 35°C data set exhibits  $\langle d_p \rangle$  that range from a low of 2  $\mu\text{m}$  at 6 ml/min to as high as 2.6  $\mu\text{m}$  at 12 ml/min. The 47°C data set has  $\langle d_p \rangle$  which are all intermediate between the 35°C and 65°C data.

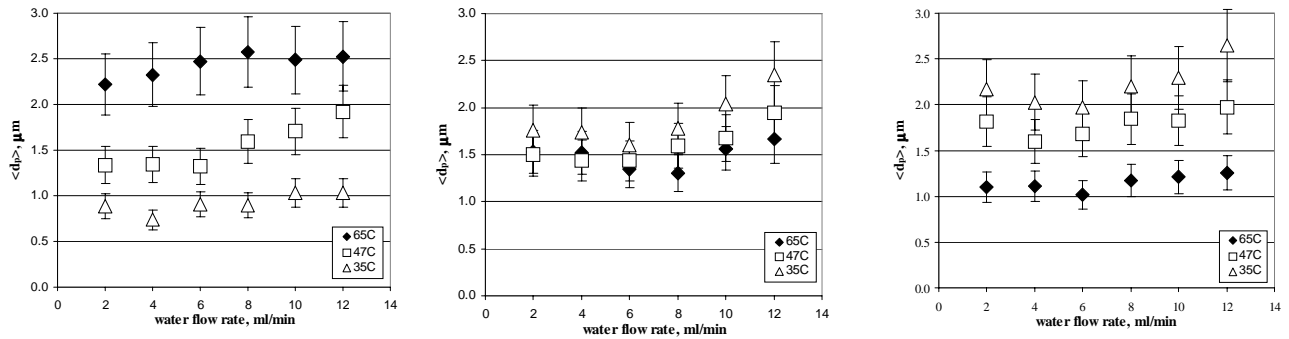


**Figure 7.** Effect of temperature on droplet size at 2.7 kV/cm and 133 Hz. (a) at 10.34 MPa, (b) at 13.79 MPa, (c) at 17.24 MPa.

Figure 8 is a plot of experimental  $\langle d_p \rangle$  versus interfacial tension data from Chun and Wilkinson.<sup>25</sup> The temperature and pressure are indicated for each data point in the plot. The data points represented by squares are slightly mismatched because the  $\langle d_p \rangle$  was measured at 47°C while the interfacial tension was measured at 40°C. A linear regression of the remaining data shows a correlation of  $\langle d_p \rangle$  with interfacial tension with a correlation coefficient ( $R^2$ ) of 0.9184, which suggests the variation in interfacial tension may be a cause of the variation of  $\langle d_p \rangle$  with state conditions. Of course, surface tension may not be the only cause for changes of  $\langle d_p \rangle$  with state conditions. Several other physical properties vary as well, including the liquid density and especially the  $\text{CO}_2$  density. In addition, electrical conductivity and dielectric constant of the fluids also change with state conditions.

## Mass Transfer.

In prior paragraphs the focus of attention has been the characterization of the electrohydrodynamic performance of the EDC by studying the effects of operating variables on  $\langle d_p \rangle$ . In subsequent work the focus shifted to using the EDC to perform an extraction of ethanol from a 10 vol. % aqueous ethanol solution using SC-CO<sub>2</sub>. The results at a condition of 35°C and 10.34 and 17.24 MPa are presented and compared to theoretical equilibrium predictions based on flash calculations using the Peng-Robinson (PR) equation of state model. Figure 9 displays the effect of increasing CO<sub>2</sub> flow rate on the separation factor,  $\alpha$ , defined as  $(y_2/x_2)/(y_1/x_1)$  where x and y denote mole fractions in the liquid and supercritical phases, respectively. Points represent the experimental data and the theoretical predictions are represented as a line. Similar results were obtained at other temperatures and pressures.

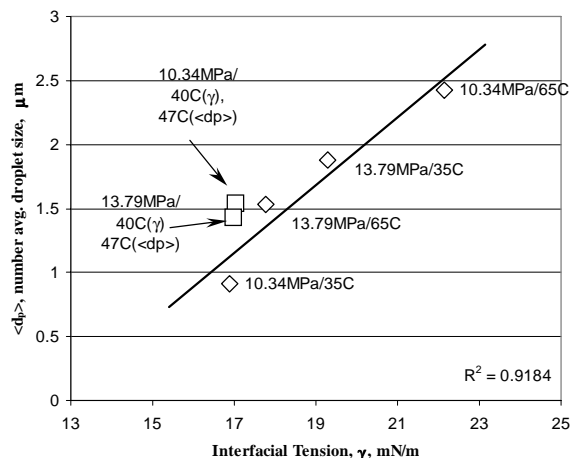


**Figure 8.** Correlation of droplet size with interfacial tension. Interfacial tension data from Chun and Wilkinson.<sup>25</sup>

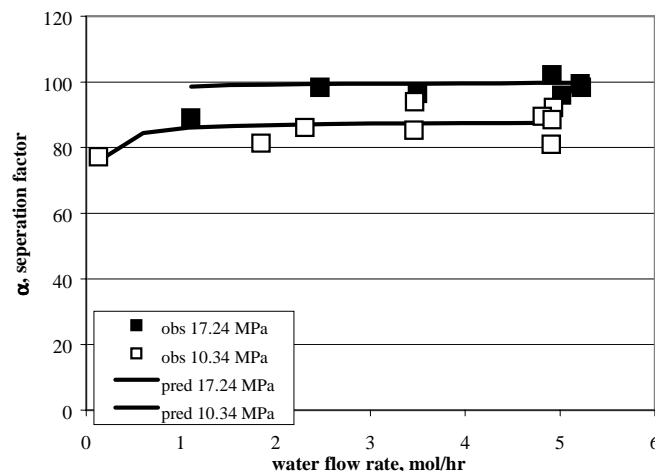


**Figure 9.** Ethanol-water separation factor for extraction of 10 vol% aqueous ethanol at 35 C, 2.7kV/cm, 133Hz, 4 ml/min.

There is an important conclusion that can be drawn from the observation that the separation achieved in the EDC is determined only by equilibrium for all conditions studied up to about 5 mol/hr CO<sub>2</sub> flow rate. Entrainment of micron-size liquid droplets from the EDC is apparently negligible; otherwise the measured extract ethanol concentration would have been lower than the equilibrium concentration. The liquid feed concentration and the liquid effluent

concentration were always much lower than the extract concentration. Any entrainment of the liquid would have decreased the measured extract concentration below the equilibrium value. It is generally believed that the micron-size droplets produced by electrospraying are electrically charged. Charged droplets would be strongly attracted to the wire mesh electrode. Apparently, a high degree of droplet coalescence at the wire mesh electrode was achieved in the EDC, resulting in negligible liquid entrainment.

Figure 10 gives the rate of extraction of ethanol and water at 10.34 MPa and 35°C. Because of the limited capacity of the condensers used to recover the extracted ethanol and water, extraction rates that would characterize the intrinsic mass transfer performance of the EDC could not be achieved in the present study. The actual mass transfer rates achieved were very modest, only up to  $1.34 \times 10^{-4}$  gmol/cm<sup>3</sup>s. In the experiments described, it has not been possible to determine the liquid phase hold up and, hence, the droplet residence time in the EDC. There is no evidence that the submicron-size dispersions are stable, indeed, the contact time in the EDC appears to be brief.

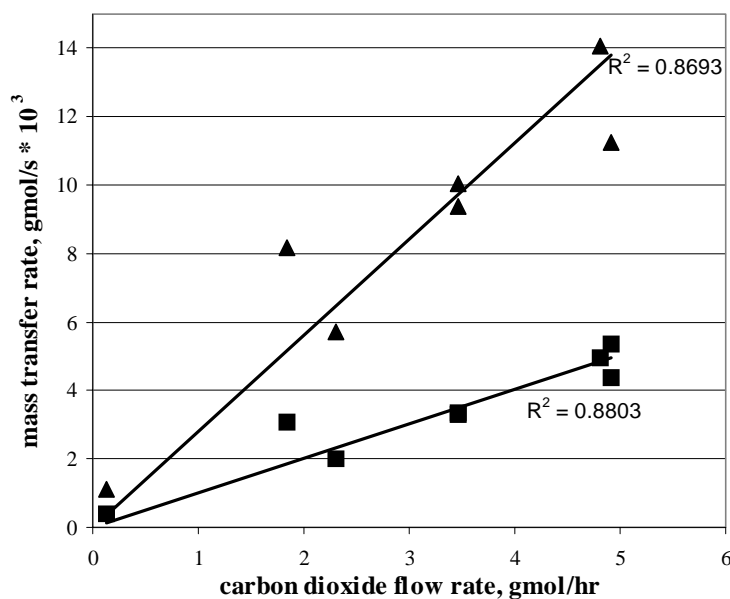


**Figure 10.** Extraction rate of ethanol (triangles) and water (squares) at 4 ml/min 10 vol% aqueous ethanol, 2.7 kV/cm, 133 Hz, 10.34 MPa, and 35C.

### **Concluding Remarks.**

This first study of electro spraying of a liquid into a dense, supercritical fluid has demonstrated a new method for dispersing aqueous liquid into SC-CO<sub>2</sub> using pulsed high-voltage electric fields. With a laser light scattering system it was possible to determine the dependence of mean droplet size on operating variables such as field strength, pulse frequency, flow rate, temperature, and pressure. Contrary to prior studies of electro spraying liquid into gas and operating in the cone-jet mode, increased field strength caused  $\langle d_p \rangle$  to increase. Likely this was the result of polydispersity in the electro spray at conditions beyond the cone-jet mode. In all cases, whether increasing flow rate or field strength, lowering the pulse frequency appeared to give smaller  $\langle d_p \rangle$ . The effect of increasing  $\langle d_p \rangle$  with increasing flow rate is consistent with results by other researchers studying electro spraying of liquid into gas.

An extraction of ethanol from a 10 vol. % aqueous ethanol solution was performed, and compared with flash calculations using the Peng-Robinson equation of state. Variation of  $\langle d_p \rangle$  correlates with surface tension, one of the several physical properties of the system that are changing with both temperature and pressure. Extraction of ethanol with the EDC was limited by equilibrium up to the highest molar flow rates of CO<sub>2</sub> achievable with the present apparatus, occurring with 100 % efficiency for a single theoretical stage with mass transfer rates up to  $1.34 \times 10^{-4}$  gmol/cm<sup>3</sup>s. Entrainment of micron-size liquid droplets from the EDC is apparently negligible; otherwise the measured extract ethanol concentration would have been lower than the equilibrium concentration. It is generally believed that the micron-size droplets produced by electrodispersion are electrically charged. Charged droplets would be strongly attracted to the wire mesh electrode. Apparently, a high degree of droplet coalescence at the wire mesh electrode was achieved in the EDC, resulting in negligible liquid entrainment.

It was hoped that CO<sub>2</sub> flow rates could be reached where much higher rates of extraction could be studied and where the ethanol extraction was mass transfer limited. Unfortunately, this was not achieved because of the limited capacity of the condensers. In future work, it would be desirable to design and install condensers capable of operating at substantially higher CO<sub>2</sub> flow rates so that the intrinsic mass transfer performance of the EDC can be studied. Since the current operation measures a number average dispersion size, it is difficult to accurately determine the total surface area in contact with the SC- CO<sub>2</sub> phase. It would be beneficial to disperse a water soluble dye so that water holdup could be measured photometrically. If it were possible to

measure the suspended liquid volume, then a calculation could be made of total surface area, which would then lead to the determination of mass transfer coefficients.

Using pulsed electric fields to produce a fine dispersion of aqueous droplets into SC-CO<sub>2</sub> appears to be an attractive possibility for improved operations where an environmentally friendly system is desired. Because the electric current in the EDC is very small,<sup>18</sup> electric power consumption per unit of surface area produced is much smaller than in conventional phase contactors. These dispersions lend themselves to a variety of applications including extractions, dyeing operations, reactions, and formation of fine particles. Likely initial commercial applications of this technology might be found for systems where a small volume of high-value product must be extracted from an aqueous medium such as might be found in the pharmaceutical industry. The present work has established a basis for broadening the range of applicability of solvent substitution by SC-CO<sub>2</sub>. It provides a means of contributing to the fundamental knowledge of droplet formation by electrodispersion in a unique experimental way since SC-CO<sub>2</sub> affords the range of variables not available in most experiments. And it offers opportunities for exploring the behavior of micro-droplets in supercritical fluids.

#### **Acknowledgments.**

We thank our colleagues V. M. Shah, D. W. DePaoli, C. Tsouris, and C. H. Byers for helpful assistance. We gratefully acknowledge support for this work from the Division of Chemical Sciences of the U. S. Department of Energy and, initially, from the ORNL Seed Money Fund. Oak Ridge National Laboratory is operated for the DOE by Lockheed Martin Energy Research Corp. under contract number DE-AC05-96OR22464.

#### **Literature Cited.**

- (1) Scott T.C.; Wham, R.M. Surface Area Generation and Droplet Size Control in Solvent Extraction Systems Utilizing High Intensity Electric Fields. **1988**, U. S. Patent No. 4,767,929.
- (2) Scott, T.C. Magnetic/Electric Field Solvent Extraction. **1989**, U. S. Patent No. 4,941,959.
- (3) Harris, M.T.; Sisson, W.G.; Basaran, O.A. Improved Nozzle for Electrical Dispersion Reactor. **1995**, U. S. Patent No. 5,464,195.
- (4) Harris, M.T., T.C. Scott, and C.H. Byers, Method and Apparatus for Preparing Metal Oxide Powders. **1992**. U.S. Patent No. 5,122,360.

- (5) Harris, M.T.; Scott, T.C.; Byers, C.H. Method and Apparatus for the Production of Metal Oxide Powder. **1993**, U. S. Patent No. 5,207,973.
- (6) Scott T.C.; Wham, R.M. An Electrically Driven Multistage Countercurrent Solvent Extraction Device: the Emulsion-Phase Contactor. *Ind. Eng. Chem. Res.*, **1989**, 28, 94.
- (7) Harris, M.T.; Scott, T.C.; Basaran, O.A.; Byers, C.H. Morphology Control in Precursor Ceramic Powder Production by the Electrical Dispersion Reactor. *Mat. Res. Soc. Symp. Proc.*, **1990**, 180, 153.
- (8) Harris, M.T.; Scott, T.C.; Basaran, O.A.; Byers, C.H. Formation of Y-Ba-Cu (1-2-3) Hydrous Oxide Precursor Powders in the Electric Dispersion Reactor. *Superconducting Engineering, AIChE Symp. Ser.*, **1992**, 88, 44.
- (9) Harris, M.T.; Sisson, W.G.; Scott, T.C.; Basaran, O.A.; Byers, C.H.; Renand, W.; Meek, T. Multiphase Electrodispersion Precipitation of Zirconia Powders. *Mat. Res. Soc. Symp. Proc.*, **1992**, 271, 945.
- (10) Harris, M.T.; Scott, T.C.; Byers, C.H. The Synthesis of Metal Hydrous Oxide Particles by Multiphase Electrodispersion. *Mat. Sci. Eng.*, **1993**, A168, 125.
- (11) Scott, T.C.; DePaoli, D.W.; Sisson, W.G. Further Development of the Electrically Driven Emulsion-Phase Contactor. *Ind. Eng. Chem. Res.*, **1994**, 33, 1237.
- (12) Harris, M.T.; Sisson, W.G.; Hayes, S.M.; Bobrowski, S.J.; Basaran, O.A. Porous Spherical Shells and Microspheres by Electrodispersion Precipitation. *Mat. Res. Soc. Symp. Proc.*, **1995**.
- (13) Scott, T.C.; Cosgrove, J.M.; DePaoli, D.W.; Sisson, W.G. Use of the Electrically Driven Emulsion-Phase Contactor for a Biphasic Liquid-Liquid Enzyme System: the Oxidation of p-Cresol in Toluene by Aqueous-Phase Horseradish Peroxidase. *Appl. Biochem. Biotech.*, **1995**, 51/52, 283.
- (14) Tang, K.; Gomez, A. On The Structure Of An Electrostatic Spray Of Monodisperse Droplets. *Phys. Fluids A*, **1994**, 6, 2317-2332.
- (15) Cloupeau, M.; Prunet-Foch, B. Electrostatic Spraying of Liquids: Main Functioning Modes. *J. Electrostatics*, **1990**, 25, 165-184.
- (16) Cloupeau, M.; Prunet-Foch, B. Electrohydrodynamic Spraying Functioning Modes - A Critical Review. *J. Aerosol Sci.*, **1994**, 25, 1021-1036.
- (17) Hayati, I., Bailey, A.I.; Tadros, T.H.F. Investigation into the Mechanisms of Electrohydrodynamic Spraying of Liquids. *J. Colloid Interface Sci.*, **1987**, 117, 205-222.

- (18) Fernandez de la Mora, J.; Loscertales, I.G. The Current Emitted By Highly Conducting Taylor Cones. *J. Fluid Mech.*, **1994**, *260*, 155-184.
- (19) Tang, K.; Gomez, A. Generation by Electrospray of Monodisperse Water Droplets for Targeted Drug-Delivery by Inhalation . *J. Aerosol Sci.*, **1994**, *25*, 1237-1249.
- (20) Fernandez de la Mora, J.; Navascues, J. Generation of Submicron Monodisperse Aerosols in Electrospays. *J. Aerosol Sci.*, **1990**, *21*, S673-S676.
- (21) Scott, T.C. Surface-Area Generation And Droplet Size Control Using Pulsed Electric-Fields. *AIChE Journal*, **1987**, *33*, 1557-1559.
- (22) Scott, T.C. *Chemical Separations, I: Principles*, C.J. King, J.D. Navratil, Eds., Litarvan: Denver 1986.
- (23) Lamb, H., *Hydrodynamics*, 6<sup>th</sup> ed., 475, Dover: N.Y., 1945.
- (24) Chen, D.; Pui, D.Y.H. Experimental Investigation of Scaling Laws for Electrospaying: Dielectric Constant Effect. *Aerosol Sci. and Tech.*, **1997**, *27*, 367-380.
- (25) Chun, B.S.; Wilkinson, G.T. Interfacial Tension in High Pressure Carbon Dioxide Mixtures. *Ind. Eng. Chem. Res.*, **1995**, *1*, 4371-4377.